



# Research on Output Stability of DC Motor Based on PD Control

Limin Sun

College of Sino-German, University of Shanghai for Science and Technology, Shanghai  
200093, China

2223030202@st.usst.edu.cn

**Abstract.** It is known to all that the application of Proportional-Derivative (PD) control is widely used in various kinds of industrial fields. This paper focus on the research of the output performance stability of the DC motor based on the PD control method. The purpose of this paper is to determine the appropriate  $K_p$  and  $K_d$  values under the circumstance that the motor transfer function from voltage to angel is determined, so that the motor has a stable and accurate output. The main methods used in this paper are simulation and mathematical calculation. To be specific, Octave is utilized to simulate to get the step response to determine the appropriate  $K_p/K_d$  and  $K_p$  values. Then Falstad is used to build a suitable circuit. During the construction, the parameter values of each component in the circuit need to be determined by mathematical calculation. When the construction is completed, the response speed and stability of the output are observed through the simulation. After that, Tinkercad is utilized to build the actual circuit and simulate it again to observe the response speed and stability of the output. In this paper, the simulated curve will be obtained. Finally the conclusions are reached: If  $K_p/K_d$  is controlled at a low value and the value of  $K_p$  is kept increasing, the fast response and low peak can be got, which is an ideal result, which has far-reaching significance for industrial development.

**Keywords:** PD control, DC motor, circuit construction

## 1 Introduction

With the widespread application of direct current (DC) motors in a wide range of industries, it is extremely crucial to ensure their performance and stability in complex control systems. Proportional-Derivative (PD) control is a common control strategy used to regulate the speed and position of DC motors. By adjusting the proportional and derivative gains, the PD controller can effectively respond to external disturbances and system nonlinearities. However, there is no doubt that the performance of a PD-controlled DC motor can be affected by factors such as parameter variations, load changes, and measurement noise. Ensuring the stability and robustness of the control system under these conditions is vital for achieving reliable

and efficient motor operation. Other researchers have used PD control in various fields, such as deformable omnidirectional mobile robots [1], flexible joint robots [2], drones [3], disinfecting robot, the CT Scanning Climbing Robot and other robot fields [4, 5], magnetic levitation system and other transportation fields [6, 7]. Researchers have delved into an array of strategies aimed at enhancing the stability and efficiency of PD-controlled DC motors, encompassing the implementation of advanced control algorithms [8], adaptive control methodologies [9, 10], and so on. By investigating the impact of these methods on the system's output stability, researchers aim to enhance the overall performance of DC motor control systems and meet the increasing demands of modern industrial applications. However, incorporating simulation and mathematical calculations to ascertain the optimal parameters has been underutilized by a majority of researchers in their studies. Therefore, further research is still necessary to investigate the correlation between PD control and the stability of performance output. The key research questions are how different PD control parameters affect the transient response, steady-state accuracy, and disturbance rejection capabilities of DC motors. By studying these questions, optimal control strategies can be identified to enhance the stability of performance output. This study aims to provide valuable insights for optimizing the design and implementation of PD control strategies in industrial applications involving DC motors. Therefore, this research carries a profound importance.

This article primarily utilizes three tools to investigate the optimal method for designing a circuit that achieves fast response without any steady state error. The conclusion which is got is that by keeping the  $K_p/K_d$  ratio low and gradually raising the value of  $K_p$ , a favorable situation arises with a rapid response and minimal peak amplitude, embodying an ideal result.

## 2 Methods and Materials

### 2.1 PD Control

The main control method in this paper is PD control. In PD control, the relationship between output voltage  $u$  and time  $t$  is as follows:  $u(t) = K_p e(t) + K_d \frac{de(t)}{dt}$ . Among them,  $K_p$  is the proportional coefficient, according to the proportional coefficient of linear adjustment system, so that the system can quickly close to the target value,  $K_d$  is the differential coefficient, this part will be differential error, to a certain extent can prevent the occurrence of excessive correction. The output voltage is closely related to the values of  $K_p$  and  $K_d$ .

The output curve of PD control will change with the change of  $K_p$  and  $K_d$  parameters, and if the parameters are not adjusted well, the result even can not meet the requirements of the control target. Therefore, how to adjust the values of  $K_p$  and  $K_d$  to achieve the ideal output is the key to the problem.

## 2.2 Transfer Function of Closed-loop Control System

The schematic diagram of the closed-loop control system is shown in Fig. 1.  $R(s)$  is the reference,  $Y(s)$  is the output,  $C(s)$  is the controller,  $P(s)$  is the plant. The derivation of the transfer function is as follows:

$$Y(s) = [R(s) - Y(s)]C(s)P(s) \quad (1)$$

$$Y(s) + Y(s)P(s)C(s) = R(s)P(s)C(s) \quad (2)$$

$$Y(s)[1 + P(s)C(s)] = R(s)P(s)C(s) \quad (3)$$

So the transfer function is:

$$\frac{Y(s)}{R(s)} = \frac{P(s)C(s)}{1+P(s)C(s)} \quad (4)$$

In this paper, PD control system is regarded as the main research object, so the whole paper takes  $P(s)$  as following transfer function as an example.

$$\frac{Angle_{out}}{Volt_{in}} = \frac{3}{0.1s^2+s} \quad (5)$$

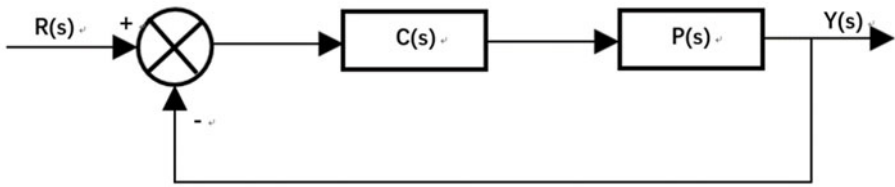


**Fig. 1.** The schematic diagram of the closed-loop control system (Photo credited: Original)

## 2.3 Methods

In this study, a comprehensive array of tools is harnessed to facilitate the research process. Octave, Falstad, and Tinkercad emerges as pivotal instruments in the exploration and analysis of circuit dynamics. The research method is shown in Fig. 2. By using Octave, the value of  $k_d$  and  $k_p$  can be determined. Then according to the parameters which be determined in Octave, the circuit can be built with Falstad, and a simulation result can be obtained. Building upon the simulation results obtained from Falstad, the research seamlessly transitions to Tinkercad for practical implementation. Here, a physical circuit is meticulously assembled using breadboards and assorted electronic components, mirroring the virtual circuit designed in Falstad. And another round of simulation is conducted in Tinkercad, providing a tangible validation of the theoretical findings.



**Fig. 2.** Flowchart of the overall approach (Photo credited: Original)

**Parameter Determination.** A tool called Octave can be utilized to analyse. The purpose of adjusting the parameters in the PD control with Octave is to enhance the responsiveness of the circuit while maintaining stability in its steady state operation. This adjustment involves fine-tuning the values of  $K_d$  and  $K_p$ . By utilizing tools such as the rlocus and pzmap functions, the position of the root and pole-zero map of the system can be visualized. This visualization aids in ensuring that the roots are within the desired region of stability, typically on the unit circle. The goal of this adjustment is to achieve a faster response time from the circuit while keeping the gain values within an acceptable range, thereby optimizing the overall performance of the system.

### Circuit Construction In Falstad.

*Transfer Function Of DC Motor.* The circuit diagram is shown in Fig. 3.

$$V = IR + L \frac{di}{dt} + K_e \omega \quad (6)$$

Because of the steady state,

$$V = IR + K_e \omega \quad (7)$$

$$I = \frac{V - K_e \omega}{R} = \frac{J \omega}{K_t} \quad (8)$$

$$JR \omega + K_t K_e \omega - K_t V = 0 \quad (9)$$

$$\frac{JR}{K_t K_e} \omega + \omega - \frac{1}{K_e} V = 0 \quad (10)$$

$$\Omega = \frac{\omega}{V} = \frac{K_m}{\tau s + 1} \left( \tau = \frac{JR}{K_t K_e}, K_m = \frac{1}{K_e} \right) \quad (11)$$

The motor transfer function from voltage to angle is:

$$\frac{Angle_{out}}{Volt_{in}} = \frac{3}{0.1s^2 + s} \quad (12)$$

So the transfer function of the DC motor is:

$$\frac{3}{0.1s + 1} \quad (13)$$

The transfer function of the integrator is:

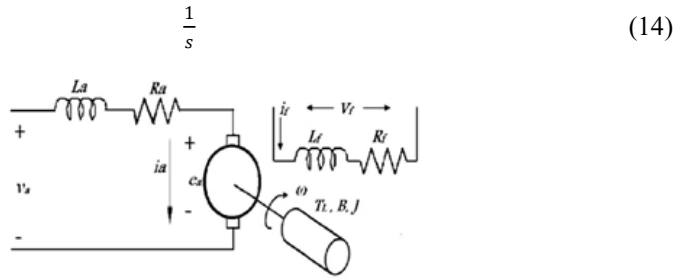


**Fig. 3.** The circuit diagram (Photo credited: Original)

*Circuit construction.* When configuring a differential amplifier, an intricate interplay of components defines the amplification process. By aligning the negative input with resistor  $R_{in}$  in series, and the positive input and output with resistor  $R_f$  in parallel, a reverse amplification factor of  $\frac{R_f}{R_{in}}$  is achieved. This setup ensures precise signal amplification within the circuit. The transfer function of a DC motor, denoted as

$$\Omega = \frac{\omega}{V} = \frac{K_m}{\tau s + 1} \tag{15}$$

Another representation of this function is:

$$\frac{V_{out}}{V_{in}} = -\frac{R_f}{R_1 R_f C_f s + 1} \tag{16}$$

To construct such an expression, the negative input and resistor  $R_1$  of the differential amplifier are in series, and the negative input and output are in parallel with the capacitor  $C_f$  and the resistor  $R_f$ . To establish an expression that relates the output voltage to the input voltage in an integrator, there is an equation:

$$v_0 = -\frac{1}{R_1 C_f} \int_0^t V_{in} dt \tag{17}$$

This equation underscores the integral relationship between input and output voltages. By connecting the negative input of the differential amplifier in series with resistor  $R_1$ , and linking the negative input and output in parallel with capacitor  $C_f$ , a circuit conducive to the desired signal processing is achieved. If the goal is to add the input voltages, then two equivalent resistors need to be connected in parallel, the negative input and output of the differential amplifier are connected in parallel with the equivalent resistance, and then the two parts are connected in series to fulfill the intended functionality. By the above methods, the desired circuit can be built.

**Circuit Construction In Tinkercad.** Tinkercad is a modeling tool employed for the creation and simulation of circuits. According to the circuit established in Falstad, the circuit is built with breadboard and other components in Tinkercad. Subsequently, the circuit is meticulously crafted and simulated to evaluate its performance and efficacy.

This meticulous approach ensures that the circuit functions optimally and meets the desired specifications.

### 3 Results

#### 3.1 Octave

The value of  $K_p$  can be determined by adjusting the ratio  $K_p/K_d$  such that the location of the root falls within the bounds of the circle, illustrated in Fig. 4. The red dot in Fig. 4 represents the optimal  $K_p$  value corresponding to the given  $K_p/K_d$  ratio. By fine-tuning this ratio, it can be ensured that the system's stability and performance characteristics meet the desired specifications, allowing for effective control and response in the system.

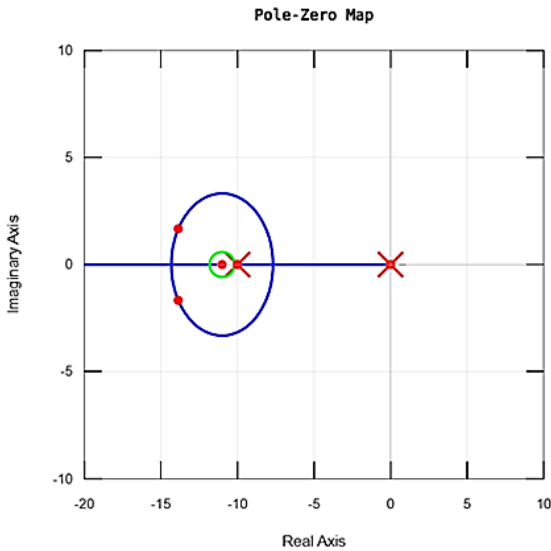


**Fig. 4.** Pole-zero Map (Photo credited: Original)

Upon completion of the simulation, the experimental data reveals the optimal value of  $K_p$  corresponding to a specific set of  $K_p/K_d$  values, as depicted in Table 1. This data provides crucial insights into the system's behavior and performance under varying control parameter configurations, helping to identify the most effective  $K_p$  value for achieving the desired control objectives.

**Table 1.** The value of  $K_p$  and the corresponding value of  $K_p/K_d$

$K_p/K_d$	10.5	11	12	13	14	15	16
$K_p$	5.3	6.5	9.5	12	15	18	22

To evaluate the response speed and peak amplitude, it is essential to analyze the step function for each parameter. In Fig. 5, the blue, red, green, and black step curves

correspond to  $K_p/K_d$  ratios of 10.5, 11, 12, and 13, respectively. Similarly, in Fig. 6, the red, blue, and green step curves represent  $K_p/K_d$  ratios of 14, 15, and 16. An optimal motor system should exhibit a swift response with minimal peak amplitude. Therefore, after careful consideration, the values  $K_p=9.5$  and  $K_p/K_d=12$  have been selected as they align with the desired system performance criteria.

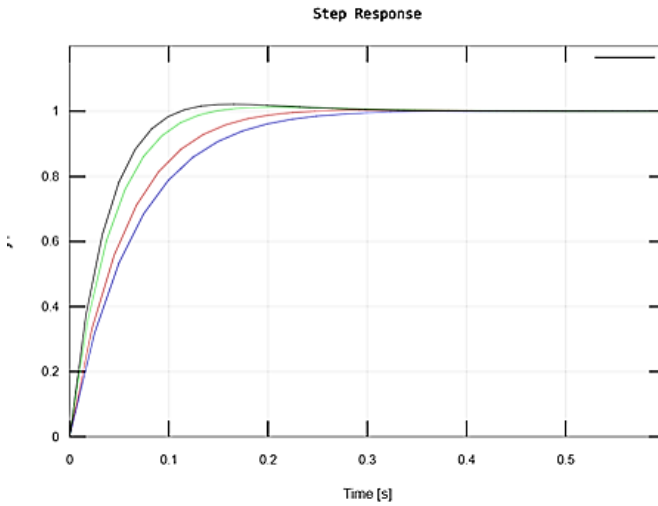


**Fig. 5.** The step response of the  $K_p/K_d$  ratios of 10.5, 11, 12, and 13 (Photo credited: Original)

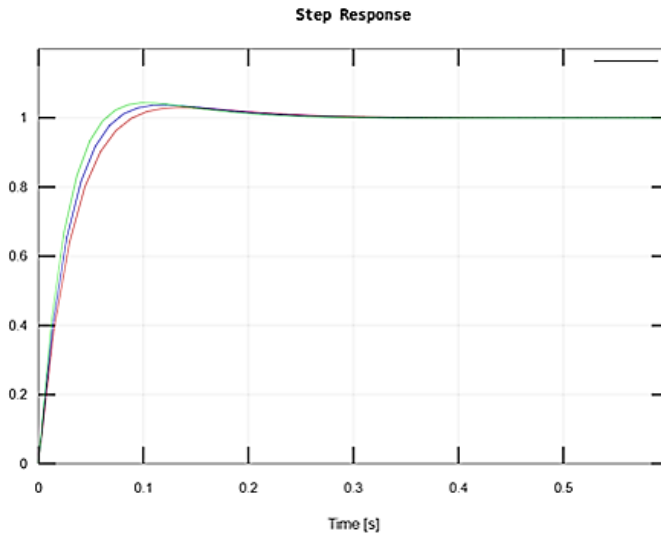


**Fig. 6.** The step response of the  $K_p/K_d$  ratios of 14, 15, and 16 (Photo credited: Original)

### 3.2 Falstad

Based on the calculated values of  $K_p = 9.5$  and  $K_p/K_d = 12$  in Octave, the derivative gain  $K_d$  is determined to be 0.792. Subsequently, the parameters of the components in the PD control circuit are set accordingly:  $R_i = 1k\Omega$ ,  $R = 9.5k\Omega$ ,  $L = 792H$ . The PD control circuit and DC motor circuit are then individually assembled following the method part of Circuit construction in Falstad in the previous section. Finally, these circuits are interconnected in series to establish an integrated circuit model that represents the ideal system configuration for further analysis and testing. The complete circuit diagram is shown in Fig. 7.

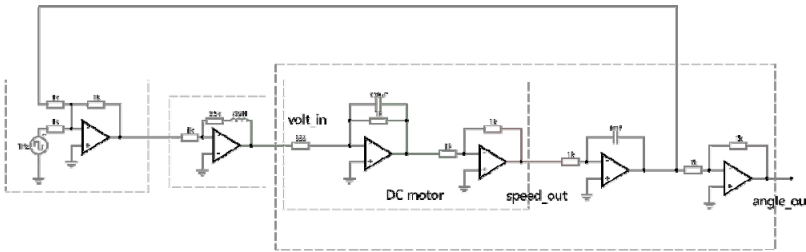


**Fig. 7.** The complete circuit diagram in Falstad (Photo credited: Original)

Through the simulation of the assembled circuit, detailed results can be obtained and analyzed. Fig. 8 illustrates the simulation results of the voltage input-angle output, and speed output. The data showcased in these figures offer valuable insights into the circuit's performance characteristics and behavior under specific operating conditions. Notably, the simulation results demonstrate a remarkable level of stability within the circuit, indicating its robust and reliable operation for the intended application.



**Fig. 8.** The simulation results of the voltage input-angle output, and speed output (Photo credited: Original)

### 3.3 Tinkercad

Following the construction of the circuit using Falstad, a corresponding implementation is carried out in Tinkercad utilizing breadboards. The specific construction results are shown in Fig. 9. Subsequently, the circuit undergoes simulation, and the resulting data is visualized through an oscilloscope. Notably, the oscilloscope display indicates that the circuit achieves stability within a mere 0.2 seconds, showcasing rapid response characteristics. Furthermore, the simulation reveals that the overshoot phenomenon is nearly imperceptible, aligning closely with the anticipated outcomes derived from both theoretical analysis and simulation exercises.



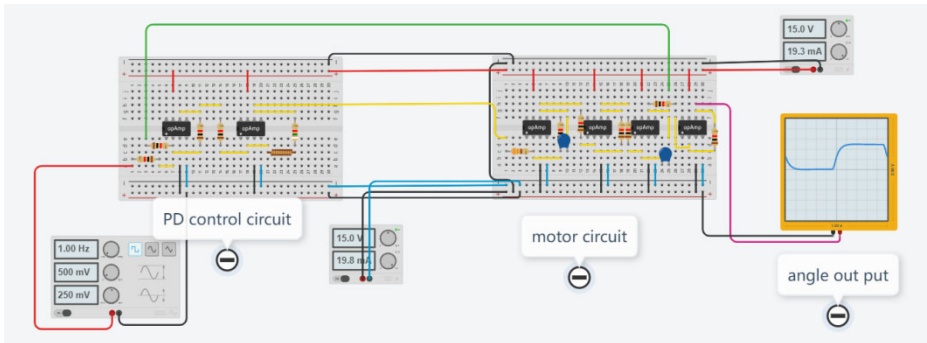


**Fig. 9.** The complete circuit diagram in Tinkercad (Photo credited: Original)

## 4 Conclusion

Upon analysis using Octave, a crucial insight is revealed: by maintaining a lower  $K_p/K_d$  ratio and incrementally increasing the value of  $K_p$ , an optimal scenario emerges with a swift response and minimal peak amplitude, representing an ideal outcome. It becomes evident that the gain values must be carefully managed within a reasonable range to prevent circuit instability during simulation. Given the inability to simulate every parameter scenario for comparison, a pragmatic approach is adopted to identify multiple sets of viable parameters for PD control tailored to specific problem contexts. Furthermore, in Falstad simulations, the circuits exhibit minimal overshoot and rapid stabilization times, showcasing exceptional performance metrics. In Tinkercad simulations, diverse application scenarios emerge based on varying parameter configurations. For instance, a lower peak amplitude can enhance circuit safety in certain contexts, underscoring the need for distinct optimal parameter settings to meet specific requirements effectively.

Undoubtedly, while the current circuit configuration demonstrates stability and accuracy, there exists the possibility of devising more streamlined circuits that can achieve comparable levels of performance. For instance, exploring alternative designs with fewer differential amplifiers or implementing novel approaches could potentially yield equally stable and error-free outcomes. This avenue of investigation presents an intriguing opportunity for further exploration and research, with the potential to uncover innovative solutions that optimize circuit efficiency and effectiveness.

## References

1. Yu, T., Zhao, LY.: Research on adaptive robust PD control for deformable omnidirectional mobile robot. *Journal Of Tianjin University Of Technology*. **39**, 1-9 (2024)
2. Guo, JC., Niu, JC., Xie, BB.: Improved Fuzzy Adaptive Compensator Based PD Control for Flexible-Joint Robot. *Machine Tool & Hydraulics*. **51**(3), 1-5 (2023)

3. Liu, WL., Pan, ZS., Cui, KK.: UAV trajectory tracking based on PD control algorithm and Isight coefficient optimization. *Journal of Ordnance Equipment Engineering*. **43**(12), 188–193 (2022)
4. Wang, D., Zhang, J., Qi, P., Zou, KK.: Research on fuzzy PID control of DC motor speed of disinfection robot. *Journal of Chongqing Technology and Business University(Natural Science Edition)*. **51**(3), 1–11 (2024)
5. Liu, CG., Zhou, YC., Liu, XP., Zhang, LB., Liu, cz.: Fuzzy PID Force Control Algorithm for the CT Scanning Climbing Robot. *SCIENTIA SILVAE SINICAE*. **54**(11), 104–110(2018)
6. Lin, HJ., Cai, ZY., Deng, DN., Wang, XZ., Huang, JX.: An adaptive fuzzy PD control method for push-down maglev. *Electronic Design Engineering*. **32**(2), 27–30+35 (2024)
7. Wang, D., Zhang, J., Qi, P., Zou, KK.: Research on fuzzy PID control of DC motor speed of disinfection robot. *Journal of Chongqing Technology and Business University(Natural Science Edition)*. **51**(3), 1–11 (2024)
8. Liu, CL., Feng, JL.,Zhang, J.: Based on Improved PD of LESO Quadrotor Control Algorithm. *Computer simulation*. **40**(6), 42–46 (2023)
9. Li, J.: Adaptive Synchronous Control Technology for Servo Position of Variable Amplitude Hydraulic Cylinder Based on Fuzzy PID. *Hydraulics Pneumatics & Seals*. **44**(3), 73-78 (2024)
10. Yu, Q., Zhang, J.: Research on Fuzzy Adaptive PID Control with Online Parameter Adjustment. *Industrial control computer*. **37**(3), 119-121+124 (2024)

**Open Access** This chapter is licensed under the terms of the Creative Commons Attribution-NonCommercial 4.0 International License (<http://creativecommons.org/licenses/by-nc/4.0/>), which permits any noncommercial use, sharing, adaptation, distribution and reproduction in any medium or format, as long as you give appropriate credit to the original author(s) and the source, provide a link to the Creative Commons license and indicate if changes were made.

The images or other third party material in this chapter are included in the chapter's Creative Commons license, unless indicated otherwise in a credit line to the material. If material is not included in the chapter's Creative Commons license and your intended use is not permitted by statutory regulation or exceeds the permitted use, you will need to obtain permission directly from the copyright holder.

